

Experimental demonstration of an analogy between optical non-coherence and irreversibility of heat transport

Aleksandr Meilakhs and Claudio Pastorino

Departamento de Física de Materia Condensada,

GIYA, CAC-CNEA, Av. Gral. Paz 1499,

San Martín, Pcia. Buenos Aires, Argentina and

Instituto de Nanociencia y Nanotecnología, INN-CONICET-CNEA

Miguel Larotonda

Laboratorio de Optica Cuántica, DEILAP,

UNIDEF (CITEDEF-CONICET), Buenos Aires, Argentina and

Departamento de Física, Facultad de Ciencias Exactas y Naturales,

UBA, Ciudad de Buenos Aires, Argentina

(Dated: May 15, 2025)

Abstract

We probe experimentally a connection between coherence in the context of optical physics and the irreversibility present in heat transfer through an interface separating two media. The robustness of the experiment on the one hand, and the theoretical description taken from the statistical-mechanics treatment of the heat transfer problem, on the other hand allows for the study of the arrow of time's problem within the clean and precise framework of experimental optical physics. The central aspect of the experiment is a light beam incident and split at an interface to produce a second common interaction point again at the interface. The experiment was carried out with two light sources that only differ in their coherence length. In the case of the highly coherent light source, we were able to combine the previously split parts of the light back into a single beam. This is indicative of the reversibility of the process of coherent light transmission through the interface. The light source with low coherence length, on the contrary, does not allow for such a recombination, thus producing an irreversible process. We explain how the latter case is analogous to the process of interfacial heat transport, thus establishing an important connection between optical non-coherence and irreversibility of transport phenomena. Our finding paves the way for the study of fundamental processes in heat transfer and the surge of irreversibility in the realm of optical physics.

I. INTRODUCTION

One of the most intriguing problems in modern physics is the irreversibility of macroscopic processes. As it was first noticed in the context of thermodynamics, the transport of heat from a hot body to a cold one gives rise to entropy production. Since entropy can only grow and never decrease such processes are irreversible [1, 2]. Later, it was found that the Boltzmann equation, along with other kinetic equations governing the behavior of large ensembles of particles are irreversible [3]. This marks a drastic contrast with the equations describing individual particles, whether in classical or quantum framework.

The most widespread approach for the derivation of the Boltzmann equation from classical mechanics is the so-called BBGKY hierarchy [4]. A serious drawback of this method is the postulate of molecular chaos, as a model for the two-particle distribution function, whose fundamentals are not properly explained. Another approach to explain entropy growth

postulates an initial low entropy state for every process. Equivalently it postulates low-entropy initial states of the universe [5, 6], which is an *ad hoc* hypothesis [7] and hence, not completely satisfactory. Some authors [8] propose modifications of the physical laws, to explicitly incorporate irreversibility.

Most modern approaches propose the emergence of irreversibility from a time-asymmetric process, which is an inherent feature of quantum physics [9]. The most studied of such mechanisms is decoherence [10, 11]. However, serious intrinsic difficulties are present in the decoherence theory [12].

In one of our previous works [13], the problem of irreversibility of heat transport through an interface between two media was addressed. It is known that a temperature jump occurs at the interface when heat flows through two different media. The proportionality coefficient between the heat flux and the temperature jump is usually called the Kapitza resistance.

Currently, the Kapitza resistance has become a wide area of research, not only for its theoretical interest, but also for its technological relevance in a wide variety of thermal management applications. Some works investigate the dynamics of the crystal lattice at the interface through computer simulations[14–19], while there is also a great number of works with analytical approaches [20–22]. Other studies deal with phonon kinetics at the interface with Boltzmann theory [23–26] or the nonequilibrium Green’s function method [27–29]. Measurements of values of Kapitza resistance for different pairs of materials were also performed [30, 31]. Additionally, the problem of Kapitza resistance was studied in a broader context than phonon transport, such as electron transport between semiconductors [32] and molecular transport at a liquid-vapor interface [33].

After the discovery of the Kapitza resistance, it was very soon realized that the temperature jump is due to the reflection of phonons at the interface [34]. Since phonon reflection at a solid-solid interface is a linear process, the Kapitza resistance effect can be used as a testbed to shed light on the mechanism that leads to irreversibility. In contrast with the time-dependent and highly non-linear Boltzmann equation, its analog at the interface between two materials, the matching equation for the distribution functions, [35, 36] is linear and static.

In Ref. [13] the interfacial phenomenon of Kapitza resistance was related to the concept of non-coherence. It was suggested that if particles incident on the interface from different sides are phase-correlated (coherent regime) then their transmission through the interface

occurs reversibly. On the contrary, if there is no phase correlation between particles at both sides of the interface (non-coherent regime), which is the naturally occurring situation, the transmission becomes irreversible. In that work, an optical experiment was proposed to clearly establish this connection between non-coherence and irreversibility. In the present manuscript we perform the suggested experiment and we empirically show the validity of this connection and the prediction of the theory [13].

The time irreversibility shown by non-coherent transmission through an interface is put to test with photons incident on an interface between two media and a two-mirror arrangement, in a conceptually simple optical experiment that implements a Mach-Zehnder interferometer [37–39]: an input light beam is split into two according to the Fresnel reflection and refraction coefficients of an air-glass interface. Different outcomes arise from the interaction of these two light beams at the same interface, determined by the coherence properties of the initial beam. With a highly coherent input beam, complete recombination into a single output beam can be achieved. In contrast, if a non-coherent source is used, a constant fraction of the light is transmitted and reflected at the interface, respectively, regardless of the prior evolution of the interacting beams¹.

In section II we present the theoretical framework within the context of light transport, an ideal experiment and a feasible experimental realization. In section III, the experimental setup is described in detail. Finally, we devote section IV to present the results and a final discussion is provided in section V.

II. THEORY

A. Preamble

We studied the light transport through an interface of two materials under two different coherence conditions of the input field, as sketched in Fig. 1. A light beam is split at a partially reflecting interface S . The reflected part of the light travels through one of the optical media and bounces at a high reflectivity surface M_1 , which is parallel to the interface. Concurrently, the refracted (transmitted) part of the light travels through a different

¹ We refer to light sources as highly coherent and non-coherent when their coherence lengths are much longer and much shorter, respectively, than the optical path difference between the two interacting beams [40].

medium and hits a second highly reflective surface M_2 . After their respective reflections, both beams are recombined at the interface. At this point, the coherence condition of the light imposes a limit on the reversibility of the process, *i.e.*, whether the light can get totally or partially recombined into a single output beam. Since the materials have different refractive indices, their relative thicknesses must be adjusted to compensate for the differing propagation lengths caused by the refraction and reflection angles. Under such condition, the second point of interaction is shared by both beams at the interface.

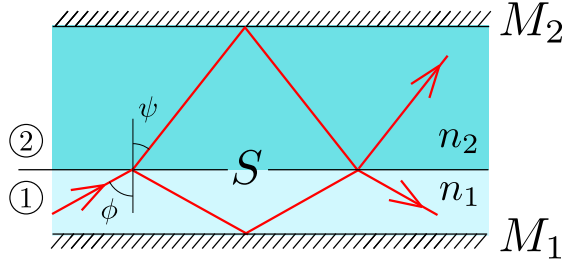


Figure 1. General scheme for the study of coherence conditions that lead to reversible and irreversible processes of photons at an interfacial boundary. Light incident on an interface S between two optical media of different refractive indexes n_1 and n_2 gets partially reflected. The refracted and reflected beams are re-routed back to the interface by means of the mirrors M_1 and M_2 , where they interact in different ways depending on the coherence condition of the light.

We consider linearly polarized waves, with a polarization perpendicular to the plane of incidence. If the light is incident on the interface from one side, the amplitudes of transmitted (refracted) and reflected light, with polarization perpendicular to the plane of incidence (s-polarization), are given by the Fresnel formula [41]:

$$r_S = \frac{\sin(\psi - \phi)}{\sin(\phi + \psi)}, \quad t_S = \frac{2 \sin \psi \cos \phi}{\sin(\phi + \psi)} \quad (1)$$

Here, ϕ and ψ are the angles between the incident and transmitted propagation directions and the axis perpendicular to the interface, respectively (Fig. 1). The interface is a boundary between two optical materials of refractive indices n_1 and n_2 . The Snell's law of refraction imposes the condition for the incident and refracted angles ϕ and ψ : $n_1 \sin \phi = n_2 \sin \psi$. For the particular condition of an interface between air and optical glass, $n_1 \approx 1$ and $n_2 = n$, hence $\sin \phi = n \sin \psi$.

If light is incident at the interface from both sides with amplitudes A_{I1} and A_{I2} , and the angles of incidence are matched by Snell's law, the amplitudes of departing waves A_{D1} , A_{D2} ,

can be found by

$$\begin{pmatrix} A_{D1} \\ A_{D2} \end{pmatrix} = \mathcal{A} \begin{pmatrix} A_{I1} \\ A_{I2} \end{pmatrix}. \quad (2)$$

where \mathcal{A} is the matrix of transformation of amplitudes defined by

$$\mathcal{A} = \frac{1}{\sin(\phi + \psi)} \begin{pmatrix} \sin(\psi - \phi) & 2 \sin \phi \cos \psi \\ 2 \sin \psi \cos \phi & \sin(\phi - \psi) \end{pmatrix}. \quad (3)$$

The values of the columns in matrix \mathcal{A} are both obtained from equation (1), with the second column assuming that the light is incident from the right direction.

In [13] it is shown that, if we normalize the amplitudes such that its squares at a given side and direction are equal to the intensity I at a given side and direction, i.e. $|A|^2 = I$, the transformation matrix becomes unitary and it is given by the following expression

$$\mathcal{U} = \frac{1}{\sin(\phi + \psi)} \begin{pmatrix} \sin(\psi - \phi) & 2\sqrt{\sin \psi \cos \psi \sin \phi \cos \phi} \\ 2\sqrt{\sin \psi \cos \psi \sin \phi \cos \phi} & \sin(\phi - \psi) \end{pmatrix}. \quad (4)$$

Throughout the remainder of the text, we will use a system of units in which squares of amplitudes represent intensities, and the transformations of amplitudes are given by unitary matrices.

It is well known that unitary matrices form a group, and for any unitary matrix, there exists an inverse matrix, which is also unitary. That is the mathematical essence of what we mean by saying transformations are reversible.

In the presented notation, the problem can be written as follows. We initially have a light beam at only one side of the interface. Let us define its amplitude as one:

$$\begin{pmatrix} A_{I1} \\ A_{I2} \end{pmatrix} = \begin{pmatrix} 1 \\ 0 \end{pmatrix}. \quad (5)$$

Upon incidence at the interface, it undergoes a transformation given by matrix \mathcal{U} (Eq. 4). Then the light is split into two parts, each of which evolves freely so that, before the next incidence on the interface, their phases will undergo the transformation $\exp(ikl)$. Here k is the corresponding wave vector and l is the distance that light travels between two instances of incidence at the interface. When the beams meet at the interface for the second time,

their amplitudes are again transformed by \mathcal{U} (see Fig. 1). So we have the following final amplitudes:

$$\begin{pmatrix} A_{F1} \\ A_{F2} \end{pmatrix} = \mathcal{U} \begin{pmatrix} e^{ik_1 l_1} & 0 \\ 0 & e^{ik_2 l_2} \end{pmatrix} \mathcal{U} \begin{pmatrix} 1 \\ 0 \end{pmatrix}. \quad (6)$$

The intensities are given by the squares of the amplitudes $|A_{F1}|^2, |A_{F2}|^2$. These intensities are ultimately measured in our experiment.

If we multiply both amplitudes on the same quantity with module 1, the resulting intensities would not change. Therefore, the important quantity that characterizes the matrix of free propagation is $\exp i(k_1 l_1 - k_2 l_2)$, *i.e.*, the phase difference between the two paths of propagation.

Since \mathcal{U} , given by Eq. (4), is symmetric then $\mathcal{U}^\dagger = \mathcal{U}$. Here the dagger symbol represents the Hermitian conjugation. We recall that the defining property of unitary matrices is $\mathcal{U}^\dagger \mathcal{U} = \mathcal{E}$, where \mathcal{E} is the identity matrix. Combining these two properties we find that $\mathcal{U}^2 = \mathcal{E}$.

If $k_1 l_1 - k_2 l_2 = 2\pi N$, for any natural value of N ($N \in \mathbf{N}$), the matrix of free propagation is equivalent to the identity matrix. This means that the product of the three matrices in the expression (6) is equal to the identity matrix: $\mathcal{U} \mathcal{E} \mathcal{U} = \mathcal{E}$. Therefore, the system that went through these series of transformations will come back to its initial state. More concretely, the two beams initially split at the interface, would merge back into a single one. That is the physical essence of the transformation being reversible.

This reasoning is valid when the light is completely coherent, or in other words, completely monochromatic. However, in reality, every light source has a finite bandwidth $\Delta\omega$ and thus a finite spectrum of wave vectors $\Delta k = \Delta\omega/c$. If $\Delta k(l_1 - l_2) \ll 1$, we can neglect the finite bandwidth and treat the light as completely coherent.

Consider the opposite, non-coherent case $\Delta k(l_1 - l_2) \gg 1$. We denote the phase difference $\Delta\phi = \Delta k(l_1 - l_2)$ and to obtain the total intensity we average over all phase differences

$$I = \frac{1}{\Delta\phi} \int_0^{\Delta\phi} d\phi |A(\phi)|^2. \quad (7)$$

By replacing the values of amplitudes from equation (6) into this expression, we obtain for

the intensity on the first side of the interface:

$$I_{F1} = \frac{1}{\Delta\phi} \int_0^{\Delta\phi} d\phi (|U_{11}|^2|U_{11}|^2 + |U_{12}|^2|U_{21}|^2 + \bar{U}_{11}U_{12}\bar{U}_{12}U_{21}e^{i\phi} + U_{11}\bar{U}_{12}U_{12}\bar{U}_{21}e^{-i\phi}). \quad (8)$$

We can write an analogous equation for the second side. If $\Delta\phi$ is large, integration of $\exp(i\phi)$ over $\Delta\phi$ yields zero. Considering this, we can write

$$\begin{aligned} I_{F1} &= |U_{11}|^2|U_{11}|^2 + |U_{12}|^2|U_{21}|^2 \\ I_{F2} &= |U_{21}|^2|U_{11}|^2 + |U_{22}|^2|U_{21}|^2. \end{aligned} \quad (9)$$

We introduce the matrix

$$\mathcal{T} = \begin{pmatrix} |U_{11}|^2 & |U_{12}|^2 \\ |U_{21}|^2 & |U_{22}|^2 \end{pmatrix}. \quad (10)$$

which, for \mathcal{U} given by expression (4), it can be written as

$$\mathcal{T} = \frac{1}{\sin^2(\phi + \psi)} \begin{pmatrix} \sin^2(\psi - \phi) & 4 \sin \psi \cos \phi \sin \phi \cos \psi \\ 4 \sin \psi \cos \phi \sin \phi \cos \psi & \sin^2(\phi - \psi) \end{pmatrix}. \quad (11)$$

Therefore, using this notation, equation (9) can be compactly written as

$$\begin{pmatrix} I_{F1} \\ I_{F2} \end{pmatrix} = \mathcal{T}^2 \begin{pmatrix} 1 \\ 0 \end{pmatrix}. \quad (12)$$

We conclude that the non-coherent case may be described in terms of intensities and their transformations by \mathcal{T} -matrices, rather than with amplitudes and their transformations by unitary matrices \mathcal{U} .

In unitary matrices, the sum of the squares of the absolute values of each element of a given row (or column) is equal to one. Since \mathcal{T} -matrices are obtained from unitary matrices by taking squares of absolute values of each element, the sum of all elements of each row (and column) is equal to one. Matrices of this type are called bistochastic. Such matrices lack inverses within this class of matrices. That is the mathematical essence of the phenomenon that is to be demonstrated: the correspondence of loss of reversibility with the loss of coherence.

From expression (12) we can see that the intensities are not dependent on the optical paths, they are strictly greater than zero, and lower than one. It means that non-coherent beams cannot be combined back into a single beam, which is the physical manifestation of the irreversibility of non-coherent transformations.

B. Scheme of the ideal experiment

Our goal is to distinguish the coherent regime from the non-coherent one. The most convenient way of observing the coherence is by measuring the visibility of the optical fringes, defined by the expression

$$\nu = \frac{I_{\max} - I_{\min}}{I_{\max} + I_{\min}}. \quad (13)$$

Experimentally, these maximum and minimum intensity values can be obtained by slightly varying the size of the air gap.

We will show experimentally that the visibility ν is zero in a non-coherent, irreversible regime, whereas it can reach values close to unity for a reversible, coherent case. In real conditions the visibility of a coherent light beam may be ultimately limited by experimental factors such as a distorted spatial mode, or scattering in the reflecting surfaces. Before reaching this condition, several aspects of the particular setup must be considered. In what follows, we describe the experimental conditions needed to obtain the highest possible degree of reversibility (maximum visibility) with the available light source.

In an “ideal” experiment, a light beam incident at a boundary between two isotropic media is split into a reflected beam and a transmitted one. These two beams are totally reflected on parallel surfaces and re-routed to a common point at the boundary surface. In order to maximize visibility, the amplitudes of both beams must be equal. These amplitudes are given by the reflection and transmission coefficients that can be obtained from Eq. (1)

Let us denote the elements of the unitary transformation matrix \mathcal{U} given by the expression in Eq. (4) as

$$\mathcal{U} = \begin{pmatrix} a & b \\ b & -a \end{pmatrix}. \quad (14)$$

The minimum intensity is obtained when the waves are incident on the interface exactly in antiphase. Therefore, the full transformation matrix (6) reads:

$$\begin{pmatrix} a & b \\ b & -a \end{pmatrix} \begin{pmatrix} 1 & 0 \\ 0 & -1 \end{pmatrix} \begin{pmatrix} a & b \\ b & -a \end{pmatrix} = \begin{pmatrix} a^2 - b^2 & 2ab \\ 2ab & -a^2 + b^2 \end{pmatrix}. \quad (15)$$

The minimum is then obtained for $a^2 = b^2$, which means that the intensities are split equally in both directions.

This results in the expression $\sin^2(\psi - \phi) = 4 \sin \psi \cos \psi \sin \phi \cos \phi$. We use the substitution $\sin \psi = n_1 \sin \phi / n_2$ and, after some manipulations, we find

$$\sin \phi = \sqrt{\frac{n_2^2 + n_1^2 - \sqrt{9/8}(n_2^2 - n_1^2)}{2}}. \quad (16)$$

This gives the incidence angle for a balanced reflection and refraction amplitudes, as a function of the refractive indices on both sides of the interface.

C. Scheme of the real experiment

However, since mirrors do not have perfect reflectivities, part of the light is absorbed by them. In order to include these losses, a more realistic transformation of the amplitudes between incident beams on the interface must include the multipliers that affect the absolute values of the amplitudes:

$$\begin{pmatrix} A_{F1} \\ A_{F2} \end{pmatrix} = \mathcal{U} \begin{pmatrix} r_1 e^{ik_1 l_1} & 0 \\ 0 & r_2 e^{ik_2 l_2} \end{pmatrix} \mathcal{U} \begin{pmatrix} 1 \\ 0 \end{pmatrix}. \quad (17)$$

and for a non-coherent transformation, we obtain

$$\begin{pmatrix} I_{F1} \\ I_{F2} \end{pmatrix} = \mathcal{T} \begin{pmatrix} R_1 & 0 \\ 0 & R_2 \end{pmatrix} \mathcal{T} \begin{pmatrix} 1 \\ 0 \end{pmatrix}. \quad (18)$$

Here, $r_1 = \sqrt{R_1}$, $r_2 = \sqrt{R_2}$, and the parameters R_1 and R_2 must be determined experimentally.

The conditions for maximal visibility is analogous to that of Eq. (15):

$$\begin{pmatrix} a & b \\ b & -a \end{pmatrix} \begin{pmatrix} r_1 & 0 \\ 0 & -r_2 \end{pmatrix} \begin{pmatrix} a & b \\ b & -a \end{pmatrix} = \begin{pmatrix} a^2 r_1 - b^2 r_2 & ab(r_1 + r_2) \\ 2ab(r_1 + r_2) & -a^2 r_1 + b^2 r_2 \end{pmatrix}. \quad (19)$$

We find that the condition of maximum visibility, which is $a^2 r_1 - b^2 r_2$ in this case, has the same physical meaning as that of the ideal case: at the recombination of beams, intensities on both sides should be equal.

Taking into account the losses due to imperfect reflection at the mirrors, it must be noticed that we will not obtain the same intensity at the output and the input. Therefore, we do not aim for the complete reversibility of the whole experiment. What we want to demonstrate is the reversibility of the process of transmission/reflection of light at the interface between the air and the glass. We achieve this by showing that all the light that is left in the system after the reflections at the mirrors, is merged into a single beam.

III. THE EXPERIMENT

A. Experimental Setup

The light source that we define as a “coherent” wave is a commercial Helium-Neon laser (Research Electro Optics model 30989, $\lambda = 632.8$ nm). The “incoherent” light source is a laser diode with a peak emission wavelength at 650 nm, driven below the threshold current, under which it behaves as a light-emitting diode (LED). In practice, there is no absolute coherent or incoherent sources. Rather, all light waves show a certain degree of temporal coherence, given by the average correlation between the wave and a delayed copy of itself. The parameter τ_c (correlation time) gives a characteristic delay for which this correlation is maintained. Correspondingly, the coherence length $\ell_c = c\tau_c$ is the distance the wave travels during the time τ_c . It is also worth noting that at the single photon level, this effect can be related to the length or duration of the photon wavepacket. The He-Ne laser has a coherence length between 10 and 30 cm, when used in the operational regime. On the other hand, the spontaneous emission from the laser diode, due to its large bandwidth, has a reduced coherence length of less than 100 μm when it is operated below the laser threshold.

To ensure equal propagation conditions, each light source was sent to a multi-axis, high-resolution fiber coupler (Thorlabs PAF-X-11-B) that allow light to be launched into a Single Mode Fiber (SMF). Therefore, the input light beam for the experiment was generated by coupling either the coherent or the incoherent source to a 2 meter SMF patchcord and sending it to the experiment using an adjustable focus fiber collimator (Thorlabs CFC-11X-B). The experiment end of the fiber patchcord was left untouched throughout the whole experiment, while the opposite end could be switched between the two fiber couplers, to select either the coherent or the incoherent light source. The purpose of the coupling and decoupling into a SMF is twofold: to obtain good beam quality by spatial filtering with the single transverse mode propagation of the fiber, and also to ensure a similar alignment for both light sources (Figure 2).

Using the adjustable lens of the collimator, we loosely focus the output beam down to a 400 μm waist at one meter from the lens, where we placed the interference experiment. A polarizing beamsplitter cube (Thorlabs PBS202) allows us to define a specific polarization for the input beam.

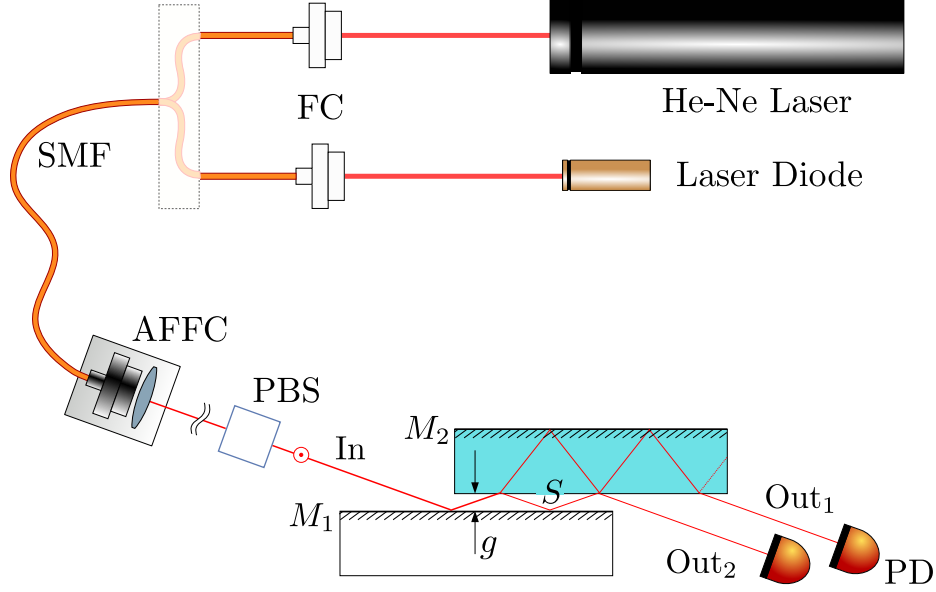


Figure 2. Experimental setup. Using a single mode fiber (SMF), we select either a coherent or an incoherent light source as the beam probe. Light is decoupled from the fiber using an adjustable focus fiber collimator (AFFC). The input polarization is selected with a polarizing beamsplitter cube (PBS). The two possible outputs are monitored with a pair of Si-biased photodetectors (PD); the intensity of the output, that propagates inside the glass is partially collected after an additional reflection in M_2 , and a transmission through the interface S . The coherent light source is a He-Ne laser, while the incoherent light source is a laser diode (LD) pumped below the lasing threshold. Each beam is sent to a fixed-lens fiber coupler (FC). This allows us to select any of the light sources by plugging the fiber patchcord into the corresponding fiber coupler. The size of the gap g controls the spatial overlap between the two beam paths.

We use a 25 mm square, 6 mm thick N-BK7 borosilicate crown-glass optical window as one of the propagating mediums ($n_2 = 1.515$). Both surfaces are optically polished and one of them has an aluminum-coating mirror deposited on it (M_2). The uncoated surface is the partially reflecting interface S between the BK7 glass and air. For the reflection in air (M_2), we use the first surface of a circular, 25 mm diameter, silver coated mirror. In this configuration, the optimum incidence angle under ideal reflectivity conditions can be calculated using the expression (16), which results in the value $\phi = 78.57^\circ$, for $n_1 = 1$ and $n_2 = 1.5151$.

Both mirrors are mounted on precision angular mounts to ensure parallelism between

surfaces. Additionally, the silver mirror mount M_1 is placed on a manual, micrometer-resolution translation stage, to allow for fine adjustment of the air gap g between the optical surfaces. This controls the overlap between both beams. By laterally displacing the two mirrors as depicted in figure 2, we gain access to the two possible outputs of the light, after the interaction between the reflected and the transmitted beams.

B. Preliminary characterization of surface reflectivities

For a coherent wave, complete reversibility with a single interaction can be expected, if the splitting ratio at the interface is close to 50% and there are similar losses on both paths. According to the previous discussions, a reflectivity of $R_S = 0.5$ can be obtained at an interface between air ($n_1 \approx 1$) and BK7 glass ($n_2 = 1.515$ for the range of wavelengths between 633 and 650 nm) for an s-polarized field and an incidence angle as large as 78.6° . This is a fairly large incidence angle, and although the transverse profile of the beam is small, it is difficult to avoid partial blocking and distortions from the edges of the mirrors. Fortunately, a mismatch between the reflectivities of mirrors M_1 and M_2 helps to avoid this problem. We measured the mirror reflectivities for the actual experimental conditions: The silver mirror M_1 has a reflectivity of $R_1 = 0.91$ for an incidence angle $\theta_i \simeq 75^\circ$, while the reflectivity of the aluminum mirror M_2 , which is deposited at the opposite surface of the BK7 slab M_2 , was measured to be $R_2 = 0.61$ for an internal incidence angle of 50° . This is, to a good approximation, the complementary angle of the refracted ray inside the glass for incidence angles between 74° and 78° . The beam propagating inside the glass suffers an increased loss, and therefore the incidence angle has to be adjusted in the experiment to obtain a larger transmissivity, which compensates for this loss imbalance, as discussed in Sec. II C.

C. Balanced loss configuration

Experimentally, we set the incidence angle at a value of $\theta_i = 76.1^\circ$ that maximizes the fringe visibility. Such angle leads to a ratio between transmissivity and reflectivity given by the Fresnel coefficients of $T_S/R_S = 1.31$ and a refraction angle $\theta_r = 39.8^\circ$. Substituting the measured reflectivities R_1 and R_2 in to the expression (19), we find that the theoretical ideal

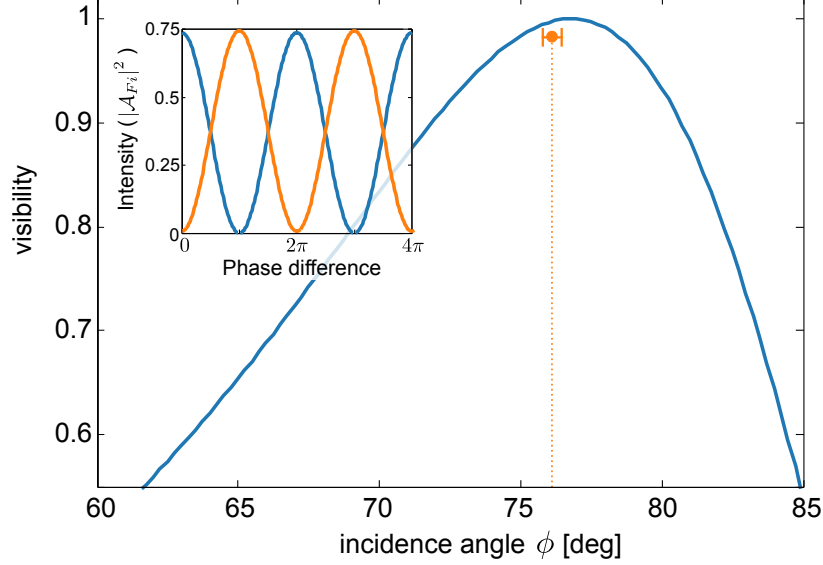


Figure 3. Measured visibility as a function of incidence angle in radians. The maximum is located at 1.34 radians, or 76.8° . In orange circular symbol is depicted the visibility value obtained experimentally. It was measured for an incidence angle of $(76.1 \pm 0.6)^\circ$. The actual visibility is affected by several factors, other than the balance of intensities, such as imperfections of the beam wavefront and scattering at the surfaces. The inset shows the calculated complimentary modulation of the intensity at both outputs, as a function of the phase difference between the two paths. This calculation considers a perfectly coherent, unit intensity input beam. The maximum output intensity departs from unity due to reflection losses.

incidence angle would be 76.8° . Remarkably, this is very close to the experimental value of 76.1° (See Fig. 3).

For such configuration, an air gap of a nominal thickness of 1.24 mm equalizes the distance traveled by both beams in the direction parallel to the interface. In this situation, depending on the coherence of the source, total recombination of the beams into a single beam may be obtained at the output. We point out that this must be understood as a signature of reversibility. Furthermore, the light can be arranged to exit the experimental setup as a single beam through either of the outputs. Depending on the phase difference between the two paths, the coherent combination of the beams will lead to constructive interference alternating between each of the outputs. This is shown in the inset of figure 3.

IV. RESULTS

After a careful adjustment of the separation g (see Fig. 2 and a careful mirror alignment, the coherent source gives rise to a complementary single-fringe interference pattern, can be observed in the two outputs. We use two large-area biased Si photodiodes (Thorlabs DET-36A) to register the light intensity at both outputs. The output that propagates in air is fully collected by the detector, while the one that propagates inside the glass is attenuated due to an internal reflection in M_2 , and a partial transmission from glass to air at the interface. This reduces the intensity by an overall factor of $R_2 T_S = 0.346$.

Figure 4 shows the normalized intensities obtained experimentally, for the input and output beams 1 and 2, as a function of the optical path length variation (OPD), obtained by changing the size of the air gap g between the two mirrors. When the coherent source is used, the relative phase between the two beams produces a complete recombination of the light in a single beam, which exits the experiment through either of the outputs. The coherent light signals are shown with full circles in Fig. 4. For OPD differences that are integers of the light wavelength ($N\lambda$, $N \in \mathbb{N}$), all the available light exits through the air side of the interface (Out₂ in Fig. 2), while for path differences that are half integers of the wavelength $(N + 1/2)\lambda$, the light is almost completely recombined on a single beam at the glass side (Out₁). The fringe visibility, calculated using Eq. (13) is above 97.5% for both outputs.

Furthermore, taking into account the additional reflections and refractions suffered by both outputs, the ideal *mean* throughput at each output can be calculated as:

$$\begin{aligned} \langle \text{Out}_1 \rangle &= R_1 (R_S T_S R_1 + R_S T_S R_2) R_2 T_S = 0.118, \\ \langle \text{Out}_2 \rangle &= R_1 (R_S^2 R_1 + T_S^2 R_2) = 0.334. \end{aligned} \tag{20}$$

These values, averaged over the phase differences, exhibit an excellent agreement with the normalized intensities obtained using the incoherent source, and they represent the mid-point of the intensity excursions obtained with the coherent light source. That aligns perfectly with our derivation of the formulas for non-coherent light by averaging over the phase differences between paths (8).

When the experiment is carried out using the incoherent light source, no intensity modulation is observed, and there is an even distribution of light at the outputs, regardless of the phase condition given by the variation of the OPD.

For comparison, the theoretical predictions for the intensities at both outputs are also shown in full lines, presenting a very good agreement with the experimental data. These are shown with plus symbols in Fig. 4.

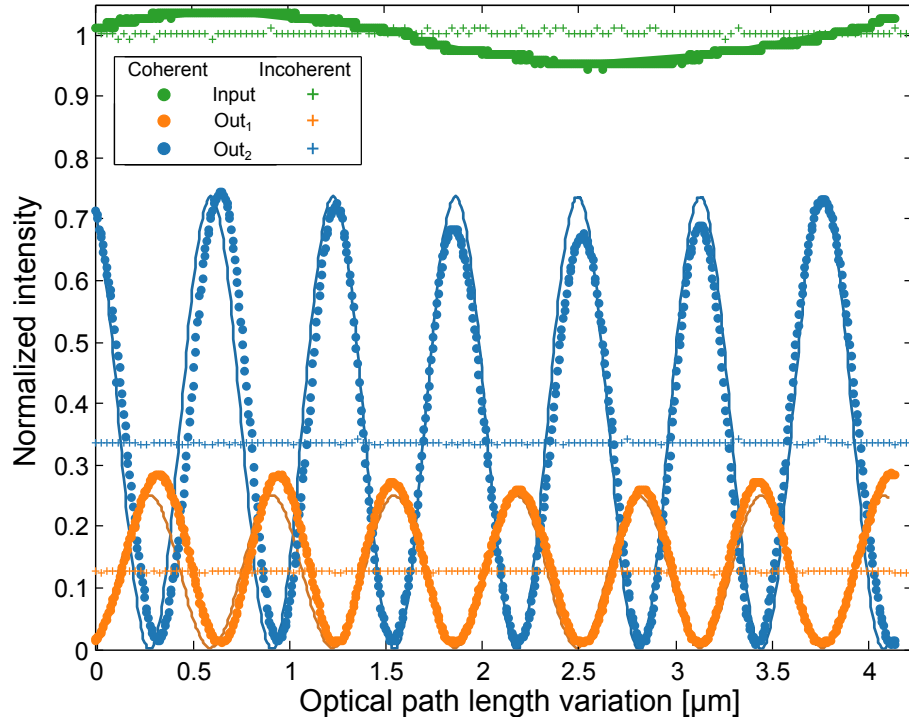


Figure 4. Measured intensities at the input and at the two complimentary outputs for both, coherent and incoherent light sources, as a function of the variation of the optical path length. The modulation was generated by changing the air gap width between the two mirrors. The coherent source shows almost ideal time reversibility when losses at the mirrors are taken into account: all the light left in the system is combined into a single beam (full circles). In contrast, when the incoherent source is used no modulation is present (plus symbols). This shows that the recombination of the two non-coherent beams always gives one result, which is half the maximum possible intensity for the coherent beams. In thin continuous lines are the theoretical predictions are shown. These were obtained by using the experimentally determined incidence angles and mirrors reflectivities measured experimentally.

Figure 4 also shows a slow varying intensity modulation in our coherent source (He-Ne laser), which is present, both, at the input and at the outputs. This effect is produced by the longitudinal modes of the laser cavity sweeping through the gain profile due to temperature-

induced variations of the laser cavity length [42]. When lasing, these modes emit with orthogonal polarization from each other and as a result, there is a polarization modulation that is observed when the laser polarization is fixed outside the cavity. Figure 4 shows a single period of such modulation during the scan of the air gap size.

It is worth to mention that, although this experiment has been carried out with intense light sources, similar results can be obtained at the single photon level. The temporal coherence, namely the length of the photon wavepacket, is inversely related to its spectral dispersion. The reversibility of the splitting at the interface within the first interaction is related to the interference at the second interaction: the fringe visibility will survive at full strength (reversible process) if the optical path difference is much smaller than the coherence length of the photon [43]. If the path difference exceeds the duration of the photon wavepacket, both contributions of the photon at the transmitted and reflected superposition state will arrive separately at the interface and the interference vanishes.

In this single-photon picture the matrices \mathcal{T} , \mathcal{U} have a different interpretation. The elements of \mathcal{T} may be interpreted as the probabilities of photon transmitting through the interface and the elements of \mathcal{U} as probability amplitudes of transmission through the interface. The difference between the coherent and incoherent regimes is understood in this case, as the regime where the transition of a photon is described by probability amplitudes with specific phase values and the regime where only the absolute value of the probability amplitude matters.

V. FINAL DISCUSSION AND CONCLUSIONS

In this work we have carried out the following an experiment that shows a strong connection between irreversibility and coherence and provide a bridge between the frameworks statistical mechanics and optical physics. In the experiment, two parts of a light beam, split by the incidence on the interface, were incident again on the interface, and met at the same spot. In the condition such that the difference between the lengths of their optical paths is much greater than the coherence length of light (non-coherent regime), the intensities measured on the outputs agree with those calculated by the formula (18). In the opposite case, when the difference between the lengths of optical paths was much shorter than the coherence length of light (coherent regime), the measured intensities that agree with those

calculated by the formula (17). In the latter case, by varying the difference between the lengths of optical paths, we were able to combine the split parts of the light back into a single beam, which confirms the reversibility of the process in the coherent regime. The non-coherent regime, on the contrary, does not allow for such a recombination, thus producing an irreversible process.

This seemingly simple optical experiment, is interpreted as an analogy to the process of heat transport through an interface. This analogy allows for studying and understanding the emergence of irreversibility in statistical-mechanics systems, in the powerful and clean framework of optical physics. If we examine different types of quantum particles such as phonons, electrons, and photons, transitioning through the interface, the equations that connect amplitudes of incident waves and departing waves take, universally, the form[13]

$$\begin{pmatrix} A_{D1} \\ A_{D2} \end{pmatrix} = \mathcal{U} \begin{pmatrix} A_{I1} \\ A_{I2} \end{pmatrix}, \quad (21)$$

where \mathcal{U} is a unitary matrix. The expressions for the elements of \mathcal{U} are different for the different types of particles and the different models, but the unitarity is universal.

From this equation, we derive another expression, that relates the distribution functions of particles departing from the interface with the distribution functions of particles incident on the interface

$$\begin{pmatrix} f_{D1} \\ f_{D2} \end{pmatrix} = \mathcal{T} \begin{pmatrix} f_{I1} \\ f_{I2} \end{pmatrix}. \quad (22)$$

Distribution functions f -s are defined as the mean number of particles in the given state, \mathcal{T} is a matrix in which the elements are probabilities of transmission or reflection of particles at the interface. The elements of \mathcal{T} are calculated as squares of absolute values of the elements of \mathcal{U} from equation (21). We call this equation a matching equation for the distribution functions.

To calculate the Kapitza resistance, we accompany the matching equations with thermalization conditions on each interface side. These conditions are needed to connect the distribution functions of particles with the temperatures at both sides of the interface. These differ by the value of the Kapitza temperature jump. In the setting of heat transport, the distribution functions of particles are not given directly, they should be expressed as functions of temperatures. In an optical setting, however, we do not have physically meaningful

analogous conditions. Instead, we point out that the intensity of light is the mean number of photons multiplied by the flux associated with each photon, $I = f\hbar\omega$, which means that the distribution of particles can be measured directly. Therefore, we only replicate the matching equations in the optical experiment.

We obtain the matching equations by finding an expression for the matrix \mathcal{T} . To this end, we need to find an explicit form for matrix \mathcal{U} . The natural way to find \mathcal{U} is by solving the following problem: let the particle be incident on the interface from one side with probability one, and find the probability amplitudes of its transmission and reflection. The solution for the case of incidence from a side 1, for example, gives the values for the first column of \mathcal{U} , while the solution for the case of incidence from side 2, gives the values of the second column (see Fig. 1). This physical situation can be also stated in a different way. Let us assume that some particle is departing from the interface on the given side with certainty, and find the probability amplitudes of its incidence from each side. By solving this problem for both sides of departure, we get the equation

$$\begin{pmatrix} A_{I1} \\ A_{I2} \end{pmatrix} = \mathcal{U}^\dagger \begin{pmatrix} A_{D1} \\ A_{D2} \end{pmatrix}, \quad (23)$$

which is mathematically equivalent to the equation (21). Indeed, it can be obtained from it, by multiplying both sides of Eq. (21) by \mathcal{U}^\dagger .

Intuitively, the equation (23) is a time-reversed version of equation (21), since the latter describes the splitting of waves at the interface, and the former the merging of two waves at the interface. Since wave equations are time-symmetric, both are equivalent. If we apply to Eq. (23) the same procedure that we used for (21), we obtain the following matching equation for the distribution functions

$$\begin{pmatrix} f_{D1} \\ f_{D2} \end{pmatrix} = \mathcal{T} \begin{pmatrix} f_{I1} \\ f_{I2} \end{pmatrix}. \quad (24)$$

By solving these equations with the same thermalization conditions, we find that for the same value of temperature difference between sides, we get the opposite values of heat flux. This means that heat flows from the colder body to the hotter body. We indeed made the time reverse.

However, equations (22) are not equivalent to (24), since $\mathcal{T} \neq \mathcal{T}^{-1}$. We started with two equivalent equations, namely Eqs. 21 and 23, applied the procedure to them, and obtained

two non-equivalent equations, i.e. Eqs. 22 and 24. Thus we have lost reversibility during the derivation of the matching equation.

In Ref. [13] was conjectured that the juncture in the derivation where the time symmetry is disrupted, is the assumption of the absence of phase correlation between particles that are incident on the interface from opposite sides. That allows for averaging over amplitude phases which, in turn, allows for the description of processes in terms of probabilities and their bistochastic transformations (11) instead of amplitudes and their unitary transformations (4). As we have pointed out before, bistochastic matrices (ignoring exceptional cases) do not have inverses, which means that they represent irreversible transformations.

The presented experimental results entirely confirm this suggestion. In the coherent regime the phase information is present, complete, and can be measured exactly, and we have found perfect reversibility. In contrast, for the non-coherent regime all the information about phases is lost and, indeed, we found that this state is irreversible. This is proved because the transformations of intensities at the interface are successfully described by bistochastic matrices (11), obtained from unitary matrices by squaring absolute values of their elements. Since intensities I and the mean number of particles f are connected by formula $I = f\hbar\omega$, they transform identically. This is exactly what we observe by comparing (12) with (22) and bearing in mind the former is a two-step transformation.

For this experiment, we have specifically employed light sources with close wavelengths and intensities (see Section III), and the only feature that accounts for the qualitative difference in the results is the coherence length of the sources.

The main difference between the experimental setting studied in this work and the case of heat transport is that the former allows to explore both, the coherent and the incoherent regimes. In a heat transport setup, the indistinguishability condition that eventually leads to interference (i.e. coherence) and reversibility is very hard to achieve. This condition involves the interaction of particles that are incident on the interface from opposite sides and hence, in a classical scenario, cannot have phase correlation. As a consequence, heat transport occurs permanently in a non-coherent regime and it is always irreversible.

We hope that this powerful analogy between coherence and reversibility, and our successful mapping from the physics of heat transfer to that of optics of beams incident in an interface, can provide a bridge between these two research areas and motivate further experimental and theoretical work. One of our goals is to include the semi-coherent case in

the presented framework. Other important route to explore is extending the scope of this analogy from interfaces to bulk materials, which can ultimately shed light on the arrow of time problem.

-
- [1] L. D. Landau and E. M. Lifšic, *Landau*, vol. 1 of *Course of theoretical physics*. Oxford: Pergamon Press, 3. ed., rev. and enl. ed., 1994.
 - [2] D. Kondepudi, *Modern Thermodynamics*. Chichester: Wiley, second edition ed., 2015. Description based upon print version of record.
 - [3] L. D. Landau and E. M. Lifshitz, *Course of Theoretical Physics*. [s.l.]: Elsevier Reference Monographs, 3. Aufl. ed., 2013. Description based upon print version of record.
 - [4] S. Harris, *An introduction to the theory of the Boltzmann equation*. Dover books on physics, Mineola, N.Y. [u.a.]: Dover Publications, 2004. Unabridged republ. of the work originally publ. by Holt, Rinehart and Winston, New York, 1971.
 - [5] S. M. Carroll and J. Chen, “Does inflation provide natural initial conditions for the universe?,” *International Journal of Modern Physics D*, vol. 14, pp. 2335–2339, Dec. 2005.
 - [6] R. M. Wald, “The arrow of time and the initial conditions of the universe,” *Studies in History and Philosophy of Science Part B: Studies in History and Philosophy of Modern Physics*, vol. 37, pp. 394–398, Sept. 2006.
 - [7] E. Cohen and T. Berlin, “Note on the derivation of the boltzmann equation from the liouville equation,” *Physica*, vol. 26, pp. 717–729, Sept. 1960.
 - [8] L. Maccone, “Quantum solution to the arrow-of-time dilemma,” *Physical Review Letters*, vol. 103, p. 080401, Aug. 2009.
 - [9] G. C. Ghirardi, A. Rimini, and T. Weber, “Unified dynamics for microscopic and macroscopic systems,” *Physical Review D*, vol. 34, pp. 470–491, July 1986.
 - [10] L. S. Schulman, *Time’s arrows and quantum measurement*. Cambridge: Cambridge University Press, 1997. Title from publisher’s bibliographic system (viewed on 05 Oct 2015).
 - [11] E. Joos, ed., *Decoherence and the appearance of a classical world in quantum theory*. Physics and astronomy online library, Berlin: Springer, 2. ed. ed., 2003. Hier auch später erschienene, unveränd. Nachdr.
 - [12] S. L. Adler, “Why decoherence has not solved the measurement problem: a response to

- p.w. anderson,” *Studies in History and Philosophy of Science Part B: Studies in History and Philosophy of Modern Physics*, vol. 34, pp. 135–142, Mar. 2003.
- [13] A. Meilakhs, “Transmission of waves and particles through the interface: reversibility and coherence,” *Annals of Physics*, vol. 466, p. 169686, 2024.
 - [14] K. Sääkilahti, J. Oksanen, J. Tulkki, and S. Volz, “Role of anharmonic phonon scattering in the spectrally decomposed thermal conductance at planar interfaces,” *Physical Review B*, vol. 90, p. 134312, Oct. 2014.
 - [15] N. Yang, T. Luo, K. Esfarjani, A. Henry, Z. Tian, J. Shiomi, Y. Chalopin, B. Li, and G. Chen, “Thermal interface conductance between aluminum and silicon by molecular dynamics simulations,” *Journal of Computational and Theoretical Nanoscience*, vol. 12, pp. 168–174, Feb. 2015.
 - [16] K. Bi, Y. Liu, C. Zhang, J. Li, M. Chen, and Y. Chen, “Thermal transport across symmetric and asymmetric solid–solid interfaces,” *Applied Physics A*, vol. 122, Sept. 2016.
 - [17] A. Alkurdi, S. Pailhès, and S. Merabia, “Critical angle for interfacial phonon scattering: Results from ab initio lattice dynamics calculations,” *Applied Physics Letters*, vol. 111, Aug. 2017.
 - [18] R. R. Kakodkar and J. P. Feser, “Probing the validity of the diffuse mismatch model for phonons using atomistic simulations,” *Physical Review B*, vol. 95, p. 125434, Mar. 2017.
 - [19] Z. Huang, C. Huang, D. Wu, and Z. Rao, “Influence of chemical bonding on thermal contact resistance at silica interface: A molecular dynamics simulation,” *Computational Materials Science*, vol. 149, pp. 316–323, June 2018.
 - [20] D. A. Young and H. J. Maris, “Lattice-dynamical calculation of the kapitza resistance between fcc lattices,” *Physical Review B*, vol. 40, pp. 3685–3693, Aug. 1989.
 - [21] L. Zhang, P. Koblinski, J.-S. Wang, and B. Li, “Interfacial thermal transport in atomic junctions,” *Physical Review B*, vol. 83, p. 064303, Feb. 2011.
 - [22] A. Meilakhs, “Phonon transmission across an interface between two crystals,” *Nanosystems: Physics, Chemistry, Mathematics*, pp. 971–982, Dec. 2016.
 - [23] A. Majumdar and P. Reddy, “Role of electron–phonon coupling in thermal conductance of metal–nonmetal interfaces,” *Applied Physics Letters*, vol. 84, pp. 4768–4770, June 2004.
 - [24] S. Merabia and K. Termentzidis, “Thermal conductance at the interface between crystals using equilibrium and nonequilibrium molecular dynamics,” *Physical Review B*, vol. 86, p. 094303, 2012.

Sept. 2012.

- [25] K. Alaili, J. Ordóñez-Miranda, and Y. Ezzahri, “Simultaneous determination of thermal diffusivity and thermal conductivity of a thin layer using double modulated thermal excitations,” *Journal of Applied Physics*, vol. 126, Oct. 2019.
- [26] G. Varnavides, A. S. Jermyn, P. Anikeeva, and P. Narang, “Nonequilibrium phonon transport across nanoscale interfaces,” *Physical Review B*, vol. 100, p. 115402, Sept. 2019.
- [27] Z. Tian, K. Esfarjani, and G. Chen, “Enhancing phonon transmission across a si/ge interface by atomic roughness: First-principles study with the green’s function method,” *Physical Review B*, vol. 86, p. 235304, Dec. 2012.
- [28] J.-S. Wang, N. Zeng, J. Wang, and C. K. Gan, “Nonequilibrium green’s function method for thermal transport in junctions,” *Physical Review E*, vol. 75, p. 061128, June 2007.
- [29] J.-S. Wang, J. Wang, and J. T. Lü, “Quantum thermal transport in nanostructures,” *The European Physical Journal B*, vol. 62, pp. 381–404, Apr. 2008.
- [30] R. M. Costescu, M. A. Wall, and D. G. Cahill, “Thermal conductance of epitaxial interfaces,” *Physical Review B*, vol. 67, p. 054302, Feb. 2003.
- [31] N. Ye, J. P. Feser, S. Sadasivam, T. S. Fisher, T. Wang, C. Ni, and A. Janotti, “Thermal transport across metal silicide-silicon interfaces: An experimental comparison between epitaxial and nonepitaxial interfaces,” *Physical Review B*, vol. 95, p. 085430, Feb. 2017.
- [32] A. P. Meilakhs, “Electronic kapitza conductance and related kinetic coefficients at an interface between n-type semiconductors,” *Journal of Physics: Condensed Matter*, vol. 36, p. 045302, Oct. 2023.
- [33] C. Pastorino, I. Urrutia, M. Fiora, and F. Condado, “Heat flow through a liquid–vapor interface in a nano-channel: the effect of end-grafting polymers on a wall,” *Journal of Physics: Condensed Matter*, vol. 34, p. 344004, June 2022.
- [34] I. M. Khalatnikov *JETP*, vol. 22, p. 687, 1952.
- [35] A. P. Meilakhs, “Nonequilibrium distribution function in the presence of a heat flux at the interface between two crystals,” *Physics of the Solid State*, vol. 57, pp. 148–152, Jan. 2015.
- [36] A. Meilakhs and B. Semak, “Calculation of kapitza resistance with kinetic equation,” *physica status solidi (b)*, vol. 258, June 2021.
- [37] P. Hariharan, *Basics of interferometry*. Elsevier, 2010.
- [38] F. Soler, “Multiple reflections in an approximately parallel plate,” *Optics communications*,

- vol. 139, no. 4-6, pp. 165–169, 1997.
- [39] V. V. Prikhodko, “Effects of multiple reflections on nonlinear absorption measurements,” *Optics Letters*, vol. 49, no. 21, pp. 6025–6028, 2024.
 - [40] M. Born and E. Wolf, *Principles of optics: electromagnetic theory of propagation, interference and diffraction of light*. Elsevier, 2013.
 - [41] E. Hecht, *Optics*. Pearson Education India, 2012.
 - [42] T. Niebauer, J. E. Faller, H. Godwin, J. L. Hall, and R. Barger, “Frequency stability measurements on polarization-stabilized he–ne lasers,” *Applied optics*, vol. 27, no. 7, pp. 1285–1289, 1988.
 - [43] R. Loudon, *The quantum theory of light*, ch. 6. OUP Oxford, 2000.